A PARAMETRIC STUDY OF HELIOSTAT SIZE FOR REDUCTIONS IN LEVELIZED COST OF ELECTRICITY

A S. Pidaparthi[1], D F. Duvenhage[2] and J E. Hoffmann[3]

[1] Solar Thermal Energy Research Group (STERG), Stellenbosch University, Private Bag X1 Matieland -7602, Stellenbosch, Western Cape, South Africa, +27 799 153 294, E-Mail: parvindsastry@gmail.com

[2] Engineering Management and Sustainable Systems research group (EMSS), Stellenbosch University, Private Bag X1 Matieland -7602, Stellenbosch, Western Cape, South Africa, +27 744 451 170, E-Mail: dfrankduv@gmail.com

[3] Senior Lecturer, Department of Mechanical Engineering, Stellenbosch University, Private Bag X1 Matieland -7602, Stellenbosch, Western Cape, South Africa, +27 218 083 554, E-Mail: hoffmaj@sun.ac.za

Abstract

Heliostats of different sizes are often compared on a 'cost per square meter' basis. This approach does not take into account other important factors like optical performance of the heliostat field, heliostat scaling and manufacturing volume effects, local weather conditions like wind speeds, possible structural deformation and the current price index. Currently, heliostats in operational power tower plants have sizes ranging from 1.14 m^2 to 150 m^2. This study aims to identify the optimum heliostat size range and aspect ratio (AR) for a hypothetical power tower plant with a net capacity of 100 MW_e and 8 hours of thermal energy storage in South Africa. Levelized cost of electricity (LCOE) is used as a figure of merit to compare heliostats of different sizes since the heliostat field contributes substantially to the capital costs of such a plant. The results indicate that a lowest theoretical LCOE value of 0.1722 USD/kWh is achieved using a 36 m^2 medium sized heliostat. The lowest LCOE values are observed with heliostats in the range of 20-40 m^2 with an AR that is greater than one. This study will be useful for power tower developers to optimally size the heliostats for their power tower plants.

Keywords: concentrating solar power (CSP); heliostat; levelized cost of electricity (LCOE); optical performance; power tower; radial-staggered.

1. Introduction

1.1. Heliostat cost reduction in power tower plants

Heliostats typically contribute to about 40% of the total installed costs in a concentrating solar power tower plant [1, 2]. Reductions in these costs can therefore considerably lower the overall costs which will directly lower the levelized cost of electricity (LCOE). This study aims to explore the subject of heliostat cost reduction by conducting a parametric study of heliostat size to determine the effect thereof on the LCOE for a power tower plant. A holistic LCOE model is suggested which compares heliostats of different sizes in a radial staggered field layout. Heliostats of different sizes are often compared on 'cost per square meter' basis which does not consider the optical performance of the heliostat field layout [3], scaling effects, impact of AR, learning curve benefits or a proper comparison of individual subcomponent cost. This study employs the method of using LCOE as a figure of merit proposed by Weinrebe et.al [4]. Figure 1 shows the major subsytems in a molten salt power tower plant.
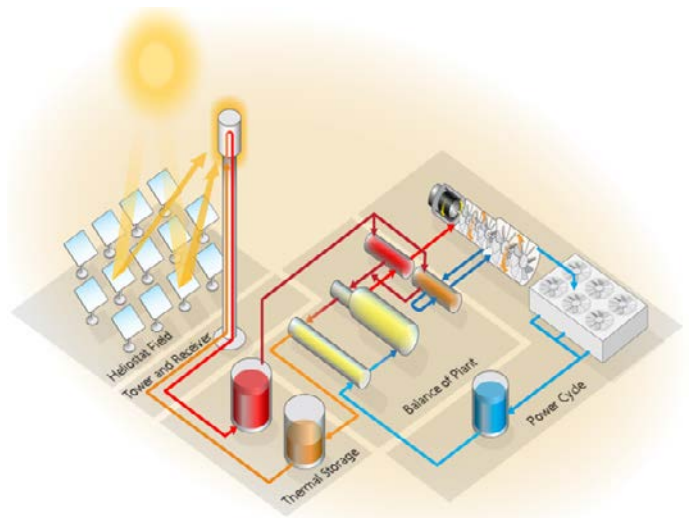
Fig. 1. Major subsystems in a molten salt power tower [5]

A major advantage with CSP, above other renewable technologies is that these plants can be combined with thermal energy storage (TES) systems [3, 4]. The high operating temperatures in power towers allow for a higher temperature differential, thus reducing the costs of TES [8]. This is essential as electricity can be produced after sunset and during peak demand hours, thereby increasing the capacity factor and the annual energy yield of the plant. This in turn has an effect on

the LCOE and profitability of the plant. The simple method for calculating LCOE to compare power plants with different technologies on the basis of cost structures and power generation, is widely accepted [9]. Power towers with several hours of TES have the potential to achieve low LCOE values and capacity factors as high as 0.80 [8]. In spite of such advantages, power towers still face challenges as they are very capital intensive. The major subsystem costs for power towers are: solar collector field, solar receiver, thermal energy storage, power block and balance of plant [10]. Heliostats are one of major cost components of power towers and it is therefore paramount to reduce heliostat costs to meet the ambitious SunShot cost objectives of reaching an LCOE of 0.06 $/kWh by the year 2020 [11]. This is essential since power towers represent 40% of the total capacity of the CSP plants currently under construction worldwide [12]. In light of these challenges, a lot of research is being done to reduce component costs for power tower plants. As of early 2016, CSP contributed 4.8 GW to the global installed generation capacity [13] and many more plants are in the construction or development phase. Spain is the world leader in terms of installed capacity with 2.3 GW of CSP plants connected to the grid [14].

1.2. Motivation

The true potential of power towers can be estimated when one considers South Africa's annual DNI values, which are as high as 3000 kWh/m^2 in some locations in the Northern Cape [15]. These values are amongst the highest in the world and are considered ideal for operating power tower plants. A study conducted in 2009 using Geographic Information Systems (GIS) indicated that South Africa has a solar and land resource potential to accommodate a nominal CSP generation capacity of 547.5 GW [16]. The results of this study however only assumed parabolic trough technology installations due to their higher maturity at that time. It is also important to note that currently power tower plants are more capital intensive than parabolic trough plants, due to lower technology maturity and greater land requirements. However, power towers are advantageous since less site preparation is needed and have higher plant efficiencies.

The first power tower plant in South Africa was commissioned in 2016 near Upington, Northern Cape. The plant, Khi solar one, is a direct steam superheated power tower plant with a net capacity of 50 MW$_e$ and approximately two hours of steam storage [17]. This plant was developed by Abengoa Solar and has 4120 heliostats, each with an aperture area of 140 m^2 [18]. These 'ASUP 140' heliostats were introduced by Abengoa in 2012 and are based on the 'SL 120' heliostats installed at the PS 10 and PS 20 plants in Spain and are expected to lower the costs of the heliostat field by approximately 30% [19]. These

heliostats will also be used in Abengoa's 110 MW$_e$ Atacama 1 power tower plant in Chile [20].

The second power tower plant in the development phase in South Africa is the Redstone solar thermal power project in Postmasburg, Northern Cape. This plant is being developed by SolarReserve and ACWA Power and is expected to start operations in 2018. The plant will have a capacity of 100 MW$_e$ with 12 hours of storage and will generate around 480 000 MWh annually [21]. There is no information yet on the heliostat size. SolarReserve's other power tower plant, Crescent dunes, in Nevada, USA, uses 'Pathfinder 2' heliostats', each with an aperture area of 62.5 m^2 [22]. The plant in Postmasburg will have a total reflective area of 1 081 250 m² with a total of 17 300 heliostats [23].

1.3. Objective

The objectives of this study are to:

- Review the range of heliostat sizes that are commercially available in the power tower market.

- Select appropriate heliostat sizes for evaluation in this study.

- Conduct a parametric study of heliostat size on SolarPILOT software to assess the optical and thermodynamic energy performance of the heliostat field layouts.

- Analyse established trends about the heliostat cost-area proportionality for the selected heliostat sizes.

- Include the optical performance, the capital costs and the annual O&M costs in a holistic LCOE model.

- Provide design recommendations for the optimum heliostat size range and AR for future 100 MW$_e$ power towers under South African conditions, based on a holistic LCOE model.

2. Approach

2.1. System design

A hypothetical power tower near Upington, Northern Cape Province in South Africa, with a net capacity of 100 MW$_e$ is evaluated in this study. The major system design parameters and the major assumptions are:

- The power tower has a net capacity of 100 MW$_e$.

- The plant has 8 hours of TES with a solar multiple of 1.8.

- Each heliostat is assumed to have 25 panels/facets arranged in a 5x5 configuration. The total heliostat width and height are varied from 3 m to 12 m so that a wide range of heliostats with different aspect ratios (width/height) are analysed.

- The solar-to-thermal efficiency of the external cylindrical receiver was set to 88%.

- The power cycle thermal-to-electric efficiency was set to 40% with dry cooling technology.

- The allowable peak flux at any point on the receiver area is assumed as 1.1 MW/m^2.

- The receiver optical height is set at 212 m for all the different heliostat field layouts.

- An external cylindrical receiver with a height of 19.49 m and a diameter of 14.64 m is used in a radial staggered heliostat field layout.

2.2. Heliostat geometry

Figure 2 illustrates the geometry of a single heliostat that defines the active reflective area used to reflect the direct beam radiation to the receiver. The total width, height and footprint diameter of the heliostat is given by W_{helio}, H_{helio} and D_{helio} respectively. The gap length between the panels in the horizontal and the vertical dimension is defined by H_{gap} and W_{gap} respectively. Similarly, $N_{panel,h}$ and $N_{panel,v}$ represent the number of panels in the horizontal and the vertical dimension respectively. All these parameters are important for calculating the active reflective area for the heliostat. The canting methods determine the orientation of each facet and an 'on-axis' canting strategy has been used throughout the analysis. The reflective surface ratio (active reflective area/total structural area) is assumed to be 0.96 for all heliostat sizes.
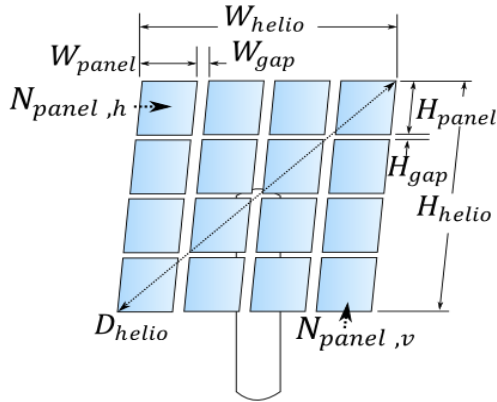
Fig. 2. Heliostat geometry definition [5]

2.3. Parametric study of heliostat size

A parametric study of heliostat size is conducted where the heliostat width and height are varied so that different heliostat sizes are analysed. A constant heliostat pedestal height of 3.5 m is assumed for all heliostat variations so that the distance between the heliostat center and the receiver optical height is kept constant [24]. The variation in the heliostat width, height and the increment value used are shown in Table 1.

Geometrical parameter	Start value	End value	Increment value
Heliostat width (m)	3	12	3
Heliostat height (m)	3	12	3

Table 1. Parametric study details for the heliostat size

Thus, a total of 16 heliostats with varying sizes and different ARs (0.5 to 4) are analysed. The smallest heliostat is 9 m^2 and the largest heliostat is 144 m^2. Heliostat sizes are categorized into three basic categories: small, medium and large. Small heliostats are in the range of 1-20 m^2, medium heliostats from 20-60 m^2 and large heliostats from 60-150 m^2. Two heliostats with the same size but different aspect ratios will have different effects on the optical performance of the heliostat field layout, hence different aspect ratios are considered. Figure 3 illustrates heliostats with the AR increasing from left to right.
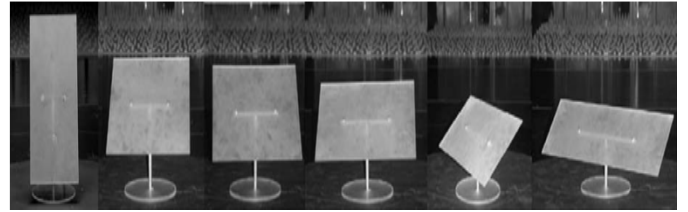
Fig. 3. Heliostats with an aspect ratio of 0.5, 1.0, 1.2, 1.5, 2.0 and 3.0 (left to right) [25]

3. Energy performance of the power tower

There are several quantities that influence the thermal power transferred to the receiver in a power tower plant. These quantities can be categorized as energetical, geometrical, and material [26]. Among these quantities, geometrical quantities can be estimated and summarized into one 'characteristic function' without major approximations [27]. This characteristic function can be defined as the effective surface area of all the heliostats, in a given field, that reflect the beam radiation onto the receiver, for a specific sun position. The geometrical quantities could relate to heliostat area or to ground area. Ground area is more useful while considering a multi-tower solar array [28]. However, this study deals with a single tower.

Leonardi and Aguanno [27] provide a simplified method to calculate the hourly intercepted energy at the receiver by multiplying the hourly DNI with the effective area of each heliostat in the field. It is assumed that each heliostat in the field has the same area. Both mirror reflectivity and soiling factor are taken as 0.95. This method has been used to develop and optimize solar field layouts in two other studies [27, 28]. The total hourly intercepted energy is expressed as follows [27]:

$$I = A_{heliostat} \times \sum_{h=1}^{8760} DNI_h \left(\sum_{i=1}^{m} \eta_{c_{i,h}} \eta_{a_i} \eta_{int_i} \eta_{s_{i,h}} \eta_{b_{i,h}} \right)$$

where, the subscript h indicates the 'hour number' and the index i represents the heliostat number with m as the total number of heliostats in the field. The subscripts c, a, int, s and b indicate cosine, atmospheric attenuation, interception/ spillage, shading and blocking efficiencies respectively [31]. These efficiencies are included in the characteristic function explained above, along with the co-ordinates of each heliostat in the field. The daylight hours from a subset of 12 representative days, selected throughout the year, is simulated so that seasonal, daily and hourly variability in the selection from a TMY3 dataset is taken into account and convergence is achieved. Figure 4 shows the nomenclature of the factors to be considered for the evaluation of the optical performance of the power tower plant.
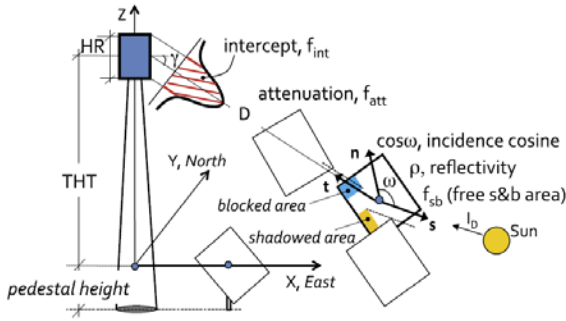
Fig. 4. Optical characterization of a power tower plant [32]

4. Heliostat field layout generation and optimization

The optical performance of the 16 heliostat sizes and the resulting field layouts is evaluated using SolarPILOT through a parametric study. SolarPILOT - Solar Power tower Integrated Layout and Optimization Tool, developed by the National Renewable Energy Laboratory (NREL) is useful for generating and optimizing heliostat field layouts. An in-built optimization algorithm is used to generate the heliostat positions and to optimize the tower height, the receiver height and the receiver AR. Several open source optimization algorithms exist and can be used for the optimization of the solar field layout. BOBYQA [33], COBYLA [34], NEWOUA [35], Nelder-Mead [36], Sbplx [37], NSPOC [38] and RSGS [39],as is the case in this study. The response surface generation methodology (RSGS) is used in this study. RSGS is an effective tool when the number of inputs in a system that must be optimized is small and the inputs are quantitative [39]. Although the number of inputs involved in the optimization of a heliostat field is quite high, the actual values to be optimized are few, i.e. the tower height, the receiver height and AR. Furthermore, these variables are all quantitative and kept constant for this study except for the

heliostat positions which are optimized.

The preliminary optimization step-size determines the first step away from the initial estimated design points and is the total fractional departure for all the variables involved. A maximum number of iterations are used until convergence is generated and the best suitable layout with the best objective function is achieved. The tolerance of the optimization determines the speed and the ease of the convergence which occurs when the objective function ceases to change during further iterations. A low tolerance takes fewer optimization steps and the objective function might not be accurate, hence a high convergence tolerance is used. The over-flux objective penalty factor is used to penalize the design when the flux intensity on the receiver exceeds the specified value of 1.1 MW/m^2. Table 2 shows the optimization settings used for the RSGS optimization algorithm in SolarPILOT.

Optimization settings	Value
Initial Optimization step size (-)	0.02
Maximum optimization iterations (-)	200
Optimization convergence tolerance (-)	0.001
Over-flux objective penalty factor (-)	0.35

Table 2. RSGS Optimization setting used for generation of the heliostat field layout

Figure 5 shows an optimized heliostat field layout generated using a medium size heliostat with an area of 43.3 m^2 and AR of 1.05. This plant has 21 290 heliostats. The solar field efficiency map shows the value for each heliostat. The colour gradient sets the lowest efficiency value to dark blue and the highest value to bright red with a corresponding transition between these extreme values.
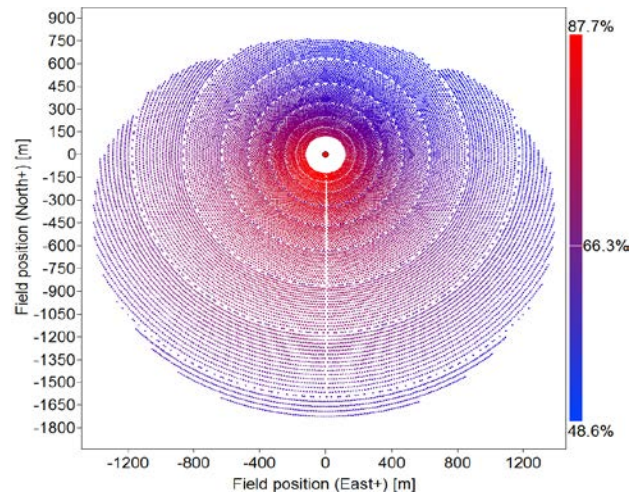
Fig. 5. Example of an optimized field with 43.3 m^2 medium size heliostats

5. Optical performance simulation

Once the optimized heliostat field layouts are generated, the optical performance of the 16 heliostat fields is simulated using the Hermite (analytical) flux simulation model. A single design point (solar noon, spring equinox) simulation is executed. Several heliostat aiming strategies exist for the cylindrical receiver [40]. The heliostat aiming strategy chosen for this study is based on the 'image size priority' method where the aim position is determined by placing the heliostat image on the receiver at points of lowest flux. The size of the image determines the order in which the heliostat images are placed on the receiver, which indicates that heliostats which are further away from the receiver will first be chosen. Table 3 shows an example of the optical performance simulation results of two heliostats of the same size but with different ARs.

Optical performance results	Heliostat with low AR	Heliostat with high AR
Heliostat width (m)	3	6
Heliostat height (m)	6	3
Heliostat total area (m^2)	18	18
AR (-)	0.5	2
Cosine efficiency (%)	81.9	83.1
Attenuation efficiency (%)	92.2	92.6
Blocking efficiency (%)	97.6	99.9
Shading efficiency (%)	100	100
Reflection efficiency (%)	90.3	90.3
Image intercept efficiency (%)	96.3	97.1
Absorption efficiency (%)	94.0	94.0
Solar field optical efficiency (%)	60.3	63.3

Table 3. Optical performance results of two heliostats with the same size but different aspect ratio

The results in this case indicate that the solar field optical efficiency is higher when the AR is higher. This is because the cosine, blocking and the image intercept efficiencies are higher. This trend, where heliostats with ARs greater than 1 have a better optical performance, is also noticed with heliostats of different sizes as seen in Fig. 6
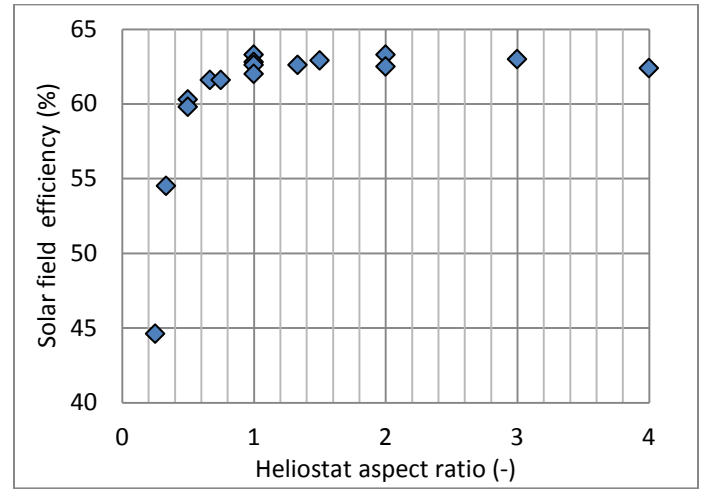
Fig. 6. Solar field efficiency as a function of aspect ratio

6. Heliostat cost as a function of size

Heliostat cost per unit for the 16 heliostats is calculated by considering the main cost categories of the heliostat: foundation, metal support structure, drives, reflector panels, and assembly of the heliostat. To evaluate these costs, a reference heliostat with a conventional pedestal/torque tube structure and an azimuth/elevation drive configuration is selected from the literature. This heliostat is chosen in such a way that it is easily scalable and recent cost information for the main cost categories is available. For this reason, a medium sized heliostat with a total area of 43.3 m^2 is chosen as the reference heliostat for this study. The specific costs for the drives and mirrors for this heliostat are based on quotations and include overhead costs and profit. An additional 20% is added to the remaining cost categories (foundations, metal support structure and assembly) to account for the business requirements of the component manufacturers [41]. Table 4 gives an indication of the heliostat cost-area proportionality for the main heliostat subcomponents considered for this study.

Table	Cost-area proportionality	Reference
Foundation	$C \propto A^{1.50}$	[42]
Metal support structure	$C \propto A^{1.47}$	[23]
Drives	$C \propto A^{0.60}$	[43]
Controls	$C \propto A^{0.2311}$	[23]
Reflector panels	$C \propto A^{1.0420}$	[23]
Assembly/Fabrication	$C \propto A^{0.426}$	[23]

Table 4. Heliostat subcomponent coat-area proportionality

7. Economic performance

7.1. Power tower cost model

The costs for the power tower have been categorized into direct and indirect capital costs. The costing model for the tower/receiver system, TES system, site preparation, and the steam and power generation system is adopted from the 2013 report 'Molten Salt Power Tower Cost Model for the System Advisor Model' to reflect the current state-of-the-art molten salt power tower technology [44]. The cost inputs for this study have been indexed to the year 2015 using the Chemical Engineering Plant Cost Index (CEPCI) from the above mentioned report. The heliostat costs have been calculated separately for the 16 different heliostats considered, and include the effects due to size scaling, learning curves benefits and the price index. The annual O&M costs are estimated separately for the heliostat fields.

7.2. Heliostat field cost model

The heliostat field costs include the foundation, metal support structure, drives, controls, mirrors and assembly costs. These costs are estimated using a reference specific cost for a single heliostat- which is then multiplied by cost effects due to scaling factor, s, effects due to high volumes accounting for learning curve benefits measured by a progress ratio, pr, and a price index, pi, reflecting the changes in heliostat sub-costs over the years. The scaling effect deals with varying heliostat sizes and is the ratio of the heliostat area under investigation, A_{hel} to that of the reference heliostat, $A^0{}_{hel}$, with s as the exponent. Learning curve effects predict the decrease in costs (or manufacturing time) with the increase in production volumes as workers in a manufacturing plant become more efficient [45]. These effects are significant for smaller heliostats since there is a percentage drop in cost with doubling of each production. These effects are accounted for using the progress ratio with the ratio of current volume of production, V_{hel} and a reference volume, $V^0{}_{hel}$ as exponent. The price index is estimated for each cost category to reflect the latest costs. However, since latest price indices for 2016 are not available for heliostats, the prices have been indexed until 2011 [23]. The total heliostat field costs, $C_{hel,tot}$, can therefore be expressed as a function of individual heliostat direct costs, $C_{hel,dir}$, and the total number of heliostats in the field, N_{hel} [23]:

$$C_{hel,tot} = C_{hel,dir} \times N_{hel}$$

where,

$$C_{hel,dir} = C_0 \times \left(\frac{A_{hel}}{A^0{}_{hel}}\right)^s \times pr^{log_2 \frac{V_{hel}}{V^0{}_{hel}}} \times pi$$

Table 5 shows the heliostat subcomponent reference costs in USD (Reference year: 2015), the progress ratio and the price index used for the calculation of the heliostat subcomponent costs.

Heliostat subcomponent cost	Reference cost/unit	Progress ratio	Price index
Foundation ($)	563.27	0.98	1.0816
Metal support structure ($)	1303.08	0.99	1.8070
Drives ($)	2030.24	0.94	1.3702
Controls ($)	62.80	0.96	1.2841
Reflector panels ($)	491.81	0.97	1.0861
Assembly ($)	701.98	0.98	1.0000

Table 5. Subcomponent reference cost, progress ratio and the price index

7.3. Annual O&M cost model

The costing model for the annual O&M expenditure is adapted from a study [44] which assumes a schedule that provides the maintenance personnel and the consumable material quantities associated with the plant. There is insufficient information in current literature about the relationship between O&M personnel required and the number of heliostats in a field. Hence a new method has been developed to estimate the O&M personnel required for the solar field while considering the suggestions from studies made in the past [16, 17]. The fixed and the variable O&M costs are estimated as per the values shown in Table 6.

O&M details	Field with large heliostats	Field with medium heliostats	Field with small heliostats
Fixed cost by capacity ($/kW-yr.)	67	68	72
Variable cost by Gen. ($/MWh)	4	4	4

Table 6. Fixed and variable O&M costs

8. Results – LCOE model

The thermo-economic performance of power tower plants depends on the optimal size of its components, and since the solar field and the TES system are the most cost intensive subsystems, they must be sized cautiously. For this reason, a parametric study is performed by increasing the solar multiple (SM) and the number of hours of TES. A study done to identify the optimum hours of storage for this plant revealed that with a SM of 3 and 16 hours of TES, capacity factors (CF) as high as 92.19% could be reached. However, upon consultation with ESKOM stakeholders, a CF constraint of 60% was recommended to determine the effect on the optimum storage capacity and investment costs [46]. Hence, in this study, the SM is fixed at 1.8 and number of hours of TES is fixed at 8. For the energy performance, hourly DNI values from the weather data have been used. This weather data uses hourly values from

a TMY3 file for Upington. The optical power is summed up during each hour for each heliostat in the field to get the annual energy reflected by the solar field to the receiver [47]. The annual energy reaching the receiver is approximated using the individual heliostat area, A_{hel}, the number of heliostats in the field, N_{hel}, the annual direct normal irradiance value, DNI, and the solar field efficiency, η_{SF}, as follows [32]:

$$E_{rec} = A_{hel} \times N_{hel} \times DNI \times \eta_{SF}$$

The net annual electrical energy generated by the plant is obtained by assuming a receiver solar to thermal efficiency, η_{Rec} of 88%, power cycle thermal-to-electric efficiency, η_{PB} of 40% and a capacity factor (CF) of 60% and is expressed as:

$$E_{PB} = E_{REC} \times \eta_{REC} \times \eta_{PB} \times CF$$

The total installed costs involved during the construction are calculated by summing up the direct and indirect capital costs. O&M costs are calculated separately based on the number of personnel required in the heliostat field configurations. The annual fuel costs are considered to be null since the plants are considered as solar only i.e. without any hybridization. Figure 7 and Fig. 8 show the LCOE results plotted against the heliostat area and the aspect ratio, respectively.
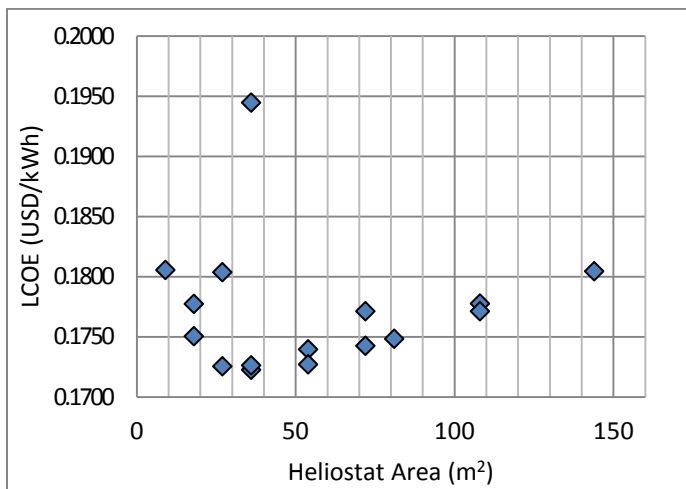
Fig. 7. LCOE as a function of heliostat area
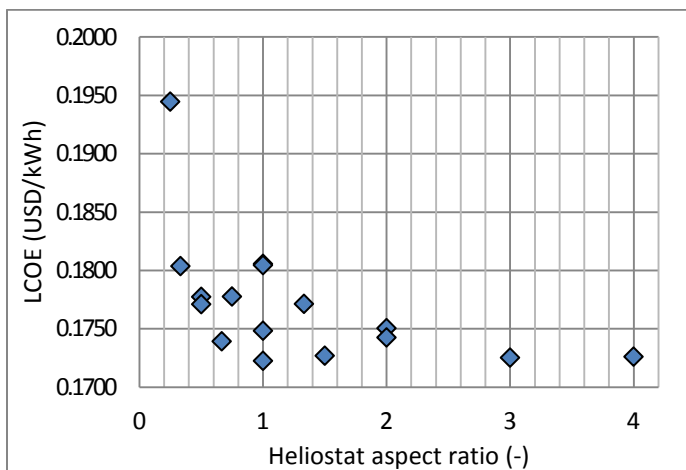
Fig. 8. LCOE as a function of heliostat aspect ratio

9. Conclusion

The theoretical framework for investigating the effects of heliostat size on the LCOE for power tower plants has been presented. Sixteen heliostats with sizes ranging from 9 m² to 144 m² and different aspect ratios are considered. The results indicate that a theoretical lowest LCOE value of 0.1722 USD/kWh is achieved for this power tower configuration using a 36 m², medium sized heliostat with an AR of 1. The lowest LCOE values are observed with heliostats in the range of 20 m² to 40 m² with ARs greater than 1. The results also indicate that heliostat 'cost per unit area' should not be taken as the sole figure of merit, but rather as a guideline while comparing heliostats of different sizes. Heliostat scaling effects, learning curve benefits, the price index and the optical performance of the heliostat field layout should also be considered while choosing the best suitable heliostat size.

References

[1] A. Pfahl, "Survey of Heliostat Concepts for Cost Reduction," *J. Sol. Energy Eng.*, vol. 136, no. 1, pp. 014501–(1–9), 2014.

[2] IRENA, "The Power to Change: Solar and Wind Cost Reduction Potential to 2025," 2016.

[3] J. N. Larmuth, W. A. Landamn, and P. Gauché, "A top-down approach to heliostat cost reduction," in *SolarPACES conference procedings 2015*, 2016, pp. 020013–1–8.

[4] G. Weinrebe, F. Von Reeken, M. Wöhrbach, T. Plaz, V. Göcke, and M. Balz, "Towards holistic power tower system optimization," in *Energy Procedia*, 2014, vol. 49, pp. 1573–1581.

[5] M. J. Wagner, "SolarPILOT User ' s Manual," 2015.

[6] R. Guédez, M. Topel, J. Spelling, and B. Laumert, "Enhancing the Profitability of Solar Tower Power Plants through Thermoeconomic Analysis Based on Multi-objective Optimization," in *Energy Procedia*, 2015, vol. 69, no. 0, pp. 1277–1286.

[7] U. Helman and D. Jacobowitz, "The Economic and Reliability Benefits of CSP with Thermal Energy Storage : Literature Review and Research Needs," 2014.

[8] L. Crespo, Z. Dobrotkova, C. Philberibert, C. Richter, G. Simbolotti, C. Turchi, and X. Wenhua, "Concentrating Solar Power," 2012.

[9] C. Kost, J. N. Mayer, J. Thomsen, N. Hartmann, C. Senkpiel, S. Philipps, S. Nold, S. Lude, N. Saad, and T. Schlegl, "Levelized Cost of Electricity Renewable Energy Technologies," 2013.

[10] G. Kolb, C. Ho, T. Mancini, and J. Gary, "Power tower technology roadmap and cost reduction plan," Albuquerque, New Mexico, 2011.

[11] U.S. Department of Energy, "SunShot Vision Study," 2012.

[12] REN21, "Renewables 2015 Global status report," (Paris: REN21 Secretaria, 2015.

[13] REN21, "Renewables 2016 Global status report," Paris, 2016.

[14] O. L. D'Ortigue, "Renewable Energy Capacity Statistics 2015," 2015.

[15] A. J. Meyer, "The South African REFIT: Solar resource assessment options for solar developers.," in *Proceedings of SASEC*, 2012, no. August 2011, pp. 1–9.

[16] T. P. Fluri, "The potential of concentrating solar power in South Africa," *Energy Policy*, vol. 37, no. 12, pp. 5075–5080, 2009.

[17] C. Silinga, P. Gauché, J. Rudman, and T. Cebecauer, "The South African REIPPP two-tier CSP tariff : Implications for a proposed hybrid CSP peaking system," in *Energy Procedia*, 2015, vol. 00.

[18] M. Geyer, "Constructing CSP Plants in the Kalahari Desert," Stellenbosch, 2014.

[19] Abengoa, "Industrial production," 2012.

[20] Abengoa, "Atacama 1: Project Brochure," 2015.

[21] SolarReserve, "Redstone Solar Thermal Power Project," 2015. [Online]. Available: http://www.solarreserve.com/en/global-projects/csp/redstone.

[22] Tonopah Solar Energy LLC, "Crescent Dunes Solar Energy Project," Santa Monica, California, 2009.

[23] G. Augsburger, "Thermo-economic optimisation of large solar tower power plants," École Polytechnique Federale de Laussane, 2013.

[24] R. Buck and E. Teufel, "Comparison and Optimization of Heliostat Canting Methods," 2009.

[25] A. Pfahl, M. Buselmeier, and M. Zaschke, "Determination of wind loads on heliostats," in *SolarPACES 2011 Conference*, 2011, pp. 1–8.

[26] F. J. Collado, "Quick evaluation of the annual heliostat field efficiency," *Sol. Energy*, vol. 82, no. 4, pp. 379–384, 2008.

[27] E. Leonardi and B. D'Aguanno, "CRS4-2: A numerical code for the calculation of the solar power collected in a central receiver system," *Energy*, vol. 36, no. 8, pp. 4828–4837, 2011.

[28] P. Schramek and D. R. Mills, "Multi-tower solar array," *Sol. Energy*, vol. 75, no. 3, pp. 249–260, 2003.

[29] S. L. Lutchman, "Heliostat Field Layout Optimization for a Central Receiver," Stellenbosch University, 2014.

[30] O. C. Scheffler, "Optimization of an Optical Field for a Central Receiver Solar Thermal Power Plant," Stellenbosch University, 2015.

[31] F. J. Collado and J. Guallar, "Campo: Generation of regular heliostat fields," *Renew. Energy*, vol. 46, pp. 49–59, 2012.

[32] F. J. Collado and J. Guallar, "A review of optimized design layouts for solar power tower plants with campo code," *Renew. Sustain. Energy Rev.*, vol. 20, pp. 142–154, 2013.

[33] M. Powell, "The BOBYQA algorithm for bound constrained optimization without derivatives," *NA Rep. NA2009/06*, p. 39, 2009.

[34] M. J. D. Powell, "Advances in Optimization and Numerical Analysis," S. Gomez and J.-P. Hennart, Eds. Dordrecht: Springer Netherlands, 1994, pp. 51–67.

[35] M. J. D. Powell, "Developments of NEWUOA for minimization without derivatives," *IMA J. Numer. Anal.*, vol. 28, no. 4, pp. 649–664, 2008.

[36] J. A. Nelder and R. Mead, "A simplex method for function minimization," *Comput. J.*, vol. 7, pp. 308–313, 1964.

[37] T. H. Rowan, "Functional stability analysis of numerical algorithms," The University of Texas at Austin, 1990.

[38] F. Ramos and L. Crespo, "a New Powerful Tool for Heliostat Field Layout and Receiver Geometry Optimization : Nspoc," *SolarPACES*, pp. 1–8, 2009.

[39] C. F. J. Wu and M. Hamada, *Experiments: Planning, analysis, and parameter design optimization*. John Wiley & Sons, INC., 2000.

[40] A. Grobler and P. Gauché, "a Review of Aiming Strategies for Central Receivers," in *Sasec 2014*, 2014, pp. 1–8.

[41] F. Von Reeken, G. Weinrebe, T. Keck, and M. Balz, "Heliostat cost optimization study," in *Conference proceedings SolarPACES 2015*, 2016, pp. 1–8.

[42] J. B. Blackmon, "Heliostat size optimization for central receiver solar power plants," in *Concentrating solar power technology: Principles, developments and applications*, Woodhead Publishing Limited, 2012.

[43] J. B. Blackmon, "Parametric determination of heliostat minimum cost per unit area," *Sol. Energy*, vol. 97, pp. 342–349, 2013.

[44] C. S. Turchi and G. a Heath, "Molten Salt Power Tower Cost Model for the System Advisor Model (SAM)," Golden, Colorado, 2013.

[45] G. F. Nemet, "Beyond the learning curve: factors influencing cost reductions in photovoltaics," *Energy Policy*, vol. 34, no. 17, pp. 3218–3232, 2006.

[46] K. Madaly, "Identifying the optimum storage capacity for a 100 - MW e concentrating solar power plant in South Africa," Stellenbosc University, 2014.

[47] J. Kunert, A. Pfahl, and R. Buck, "Dimensioning heliostat drives considering dynamic wind loads," in *SolarPaces Conference*, 2009, pp. 1–8.